Tuning of Spin Density Wave Strengths in Quasi-One-Dimensional Halogen-Bridged Ni^{III} Complexes with Strong Electron Correlations, $[Ni^{III}(chxn)_2X]Y_2$

Masahiro Yamashita,*,† Toshio Manabe,† Kazuo Inoue,† Takuya Kawashima,† Hiroshi Okamoto,‡ Hiroshi Kitagawa,§ Tadaoki Mitani,§ Koshiro Toriumi,|| Hiroshi Miyamae,⊥ and Ryuichi Ikeda⊗

Graduate School of Human Informatics and PRESTO (JST), Nagoya University, Chikusa-ku, Nagoya 464-8601, Japan, Department of Applied Physics, The University of Tokyo, Hongo, Bunkyo-ku, Tokyo 113-8656, Japan, Japan Advanced Institute for Science and Technology, Ishikawa 923-1292, Japan, Faculty of Science, Himeji Institute of Technology, Hyogo 678-12, Japan, Department of Chemistry, Jyosai University, Saitama 350-02, Japan, and Department of Chemistry, University of Tsukuba, Tsukuba 305-8571, Japan

Received October 26, 1998

A series of quasi-one-dimensional halogen-bridged Ni^{III} complexes, $[Ni(chxn)_2X]Y_2$ (chxn = 1*R*,2*R*-diaminocyclohexane; X = Cl, Br, and mixed halides; Y = Cl, Br, mixed halides, NO_3, BF_4, and ClO_4) have been synthesized in order to investigate the effect of the bridging halogens and counteranions on their crystal, electronic structures, and moreover the spin density wave strengths. In the crystal structures, the $[Ni(chxn)_2]$ moieties are symmetrically bridged by halogen ions, forming linear-chain $Ni^{III}-X-Ni^{III}$ structures. The hydrogen bonds between the aminohydrogens of chxn and the counteranions are constructed not only along the chains but also over the chains, forming the two-dimensional hydrogen-bond networks. While the $Ni^{III}-X-Ni^{III}$ distances or *b* axes are almost constant in the compounds with the same bridging halogens, the *c* axes which correspond to the interchain distances in the directions of the interchain hydrogen bonds are remarkably lengthened with the increase of the ionic radius of the counterions; $X < NO_3 < BF_4 < ClO_4$. These compounds show the very strong antiferromagnetic interactions among spins on Ni $3d_{z^2}$ orbitals through the superexchange mechanisms via the bridging halogen ions. Judging from the results of X-ray photoelectron spectra (XPS), Auger spectra, and single-crystal reflectance spectra, these Ni compounds are not Mott-insulators but charge-transfer-insulators. Their electronic structures or the spin density wave strengths are found to be tuned by the combinations of the counteranions and the bridging halogens.

Introduction

Recently, low-dimensional compounds have been attracting much attention since they show very interesting physical properties such as Peierls transition, spin-Peierls transition, neutral−ionic transition, charge density wave (CDW) states, spin density wave (SDW) states, superconductivities, etc.[1] Among these compounds, quasi-one-dimensional halogen-bridged mixed-valence metal compounds (hereafter abbreviated as MX chains) have been extensively investigated these 20 years because of their interesting physical properties such as intense and dichroic intervalence charge-transfer bands, progressive resonance Raman spectra, luminescences with large Stokes shifts, midgap absorptions attributable to solitons and polarons, large third-order nonlinear optical susceptibilities, one-dimensional model compounds of high T_c copper oxide superconductors, etc.[2]

Theoretically, the MX chains are considered as extended Peierls−Hubbard systems, where the electron−phonon interaction (*S*), the electron-transfer energy (*T*), the on-site and intersite Coulomb interactions (*U* and *V*, respectively) are competed or cooperated with one another.[3] Originally, the MX chains are considered as one-dimensional metallic states with half-filled d_{z^2} orbitals of metals and the filled pz orbitals of bridging halogens. However, as it is well-known, the one-dimensional metallic state is unstable and subsequently transferred to the insulating state by the electron−phonon interaction (*S*) and the electron correlation (*U*). In most MX chains, due to the strong electron−phonon interaction, the bridging halogens are distorted from the midpoints between the neighboring two metal atoms, giving CDW states or $M^{II}-M^{IV}$ mixed-valence states ($\cdots M^{II}\cdot\cdot X-M^{IV}-X\cdots M^{II}\cdots$). Accordingly, the half-filled metallic band is split into the occupied valence band and the unoccupied conduction band with finite Peierls gaps. These compounds are formulated as $[M^{II}(AA)_2][M^{IV}X_2(AA)_2]Y_4$ ($M^{II}-M^{IV}$ = $Pt^{II}-Pt^{IV}$, $Pd^{II}-Pd^{IV}$, $Ni^{II}-Pt^{IV}$, $Pd^{II}-Pt^{IV}$, $Cu^{II}-Pt^{IV}$; X = Cl, Br, I, and mixed halides; AA = ethylenediamine (en), 1*R*,2*R*-diaminocyclohexane (chxn), etc.; Y = ClO_4, BF_4, X, etc.). These

† Nagoya University.
‡ The University of Tokyo.
§ Japan Advanced Institute.
|| Himeji Institute of Technology.
⊥ Jyosai University.
⊗ University of Tsukuba.

(1) *Extended Linear Chain Compounds*; Miller, J. S., Ed.; Plenum: New York, 1982; Vols. I−III.

(2) (a) Yamashita, M. In *New Functional Materials, Vol. C: Synthetic Process and Control of Functionality Materials*; Tsuruta, T., Doyama, M., Seno, M., Eds.; Elsevier Science Publisher: Tokyo, 1993; p 539. (b) Bishop, A. R.; Swanson, B. I. *Los Alamos Sci.* **1993**, *21*, 133. (c) Clark, R. J. H. *Adv. Infrared Raman Spectrosc.* **1983**, *11*, 95. (d) Okamoto, H.; Yamashita, M. *Bull. Chem. Soc. Jpn.* **1998**, *71*, 2023. (e) Clark, R. J. H. *Chem. Soc. Rev.* **1990**, *19*, 107.

(3) (a) Nasu, K. *J. Phys. Soc. Jpn.* **1983**, *52*, 3865. (b) Nasu, K. *J. Phys. Soc. Jpn.* **1984**, *53*, 302. (c) Nasu, K. *J. Phys. Soc. Jpn.* **1983**, *53*, 427. (d) Gammel, J. T.; Saxena, A.; Batistic, I.; Bishop, A. R.; Phillpot, S. R. *Phys. Rev. B* **1992**, *45*, 6408. (e)Murao, T. *Physica* **1986**, *143B*, 273. (f) Nasu, K. *Physica* **1986**, *143B*, 229.

10.1021/ic9812499 CCC: $18.00
Published on Web 04/02/1999

MX chains have two characteristic points compared with the inorganic semiconductors and organic conjugated polymers as follows. The magnitudes of the band gaps or the CDW strengths can be tuned by varying chemical factors such as M, X, AA, and Y; in other words, the physical parameters (*S*, *T*, *U*, and *V*) can be tuned by substitution of the chemical factors. Moreover, the interchain interaction can be controlled by using the intra- and interchain hydrogen bonds between the aminohydrogens and the counteranions.[4] The excited states and their relaxation processes were well investigated by using various optical methods such as resonance Raman spectra, time-resolved luminescence spectra, photoinduced absorption spectra, etc.[5]

On the other hand, theoretically it was proposed that in the case of stronger on-site Coulomb interaction (*U*) compared with the electron−phonon interaction (*S*), the M^{III} state or SDW state is considered to be more stable, where the bridging halogens are located at the midpoints between neighboring two metal atoms (−X−M^{III}−X−M^{III}−X−). More recently, our groups have succeeded in synthesizing such compounds formulated as $[Ni^{III}(chxn)_2X]X_2$ (X = Cl and Br), since a Ni ion has a stronger *U* compared with that of a Pd or Pt ion and/or compared with *S* in a Ni ion.[6] These Ni compounds show very strong antiferromagnetic interaction among spins located on $3d_{z^2}$ orbital in each Ni ion through the bridging halogens. The XP spectra, Auger spectra, and single-crystal reflectance spectra have revealed that these Ni compounds are not Mott-insulators but charge-transfer-insulators, where the energy levels of the bridging halogens are located between the upper and lower Hubbard bands.[7] Therefore, the electronic structures of the Ni compounds are similar to those of the starting materials of copperoxide superconductors except for their dimensionality. While many Pt and Pd compounds were synthesized and their physical properties were extensively investigated so far, the properties of the Ni compounds have not been fully understood, since the compounds are only a few, and moreover, it is very difficult to obtain single crystals. In this study, to investigate the effect of the bridging halogens and counteranions on the SDW strengths, we have synthesized new Ni^{III} compounds, $[Ni(chxn)_2X]Y_2$ (X = Cl, Br, and mixed halides; Y = Cl, Br, mixed halides, NO_3, BF_4, and ClO_4) and investigated their crystal and electronic structures.

Table 1. Crystal Data for $Ni(chxn)_2Cl(NO_3)_2$

emp form	$[Ni(C_6H_{14}N_2)_2]Cl(NO_3)_2$
fw	446.5
cryst size(mm^3)	0.55 × 0.30 × 0.10
cryst syst	orthorhombic
a/Å	22.990(20)
b/Å	4.982(2)
c/Å	8.001(5)
V/$Å^3$	916.4(11)
Z	2
space group	*I*222
D calcd (g/cm^3)	1.618
no. of obsns	631
λ/Å	0.710 69
temp (K)	296
residuals: R^a; $R_w{}^b$	0.066,0.058

$^a R = \sum||F_o| - |F_c||/\sum|F_o|$. $^b R_w = [\sum w(F_o - F_c)^2/\sum wF_o^2]^{1/2}$.

Experimental Section

Preparation of $[Ni(chxn)_2X]X_2$ (X = Cl and Br). Single crystals of $[Ni(chxn)_2X]X_2$ were obtained by the methods previously reported.[6]

Preparation of $Ni(chxn)_2Cl_xBr_y$. Single crystals of $Ni(chxn)_2Cl_{2.459}Br_{0.541}$ and $Ni(chxn)_2Cl_{1.28}Br_{1.72}$ were obtained by slow diffusion of Br_2 and Cl_2 into the 2-methoxyethanol solutions of $Ni(chxn)_2Cl_2$ and $Ni(chxn)_2Br_2$, respectively. The ratios of Cl and Br were determined by single-crystal X-ray structure analyses as described previously.[8]

Preparation of $Ni(chxn)_2X(NO_3)_2$. Single crystals of the $Ni(chxn)_2X(NO_3)_2$ (X = Cl and Br) were synthesized by (a) chemical and (b) electrochemical methods. (a) An amount of 10 mL of 2-methoxyethanol solutions of $Ni(chxn)_2X_2$ were cooled to −10 °C, and 20 mL of 61% HNO_3 (−10 °C) was added to their solutions. They were kept in the refrigerator for 24 h, then green crystals were obtained. (b) The compounds were obtained by an electrochemical method of the 2-methoxyethanol solutions of $Ni(chxn)_2X_2$ including NH_4NO_3 as an electrolyte at room temperature with an electric current of 20 μA using an H-shaped cell.[9] The concentrations of $Ni(chxn)_2X_2$ and NH_4NO_3 were 40 mmol and 0.5 mol, respectively. After several weeks, single crystals were obtained.

Preparation of $Ni(chxn)_2X(ClO_4)_2$. The $Ni(chxn)_2X(ClO_4)_2$ (X = Cl and Br) compounds were obtained by halogenation of the 70% $HClO_4$ solutions of $Ni(chxn)_2(ClO_4)_2$ at −10 °C. Anal. Calcd for $C_{12}H_{28}N_4O_8Cl_2BrNi$: C, 25.47; H, 4.98; N, 9.97. Found: C, 25.45; H, 5.59; N, 9.45. Anal. Calcd for $C_{12}H_{28}N_4O_8Cl_3Ni$: C, 27.64; H, 5.41; N, 10.74. Found: C, 28.29; H, 5.33; N, 10.62.

Preparation of $Ni(chxn)_2Cl(BF_4)_2$. The $Ni(chxn)_2Cl(BF_4)_2$ is obtained by chlorination of the 40% HBF_4 solution of $Ni(chxn)_2(BF_4)_2$ at −10 °C. Anal. Calcd for $C_{12}H_{28}N_4F_8B_2ClNi$: C, 29.05; H, 5.68; N, 11.29. Found: C, 28.80; H, 5.45; N, 11.03.

Single-crystal X-ray structure measurement was carried out at room temperature. Intensity data were collected on a RIGAKU AFC-5 four-circular diffractometer for $[Ni(chxn)_2Cl](NO_3)_2$ using Mo Kα radiation. Crystal data are listed in Table 1. The structure was solved by the heavy atom method and refined by the full-matrix least-squares technique. All non-hydrogen atoms were refined with anisotropic thermal parameters. X-ray powder patterns were measured on MAC Science MPX3 using Cu Kα radiation at room temperature.

^{13}C CP/MAS NMR spectra of $[Ni(chxn)_2X]Y_2$ and $[Pd(chxn)_2][PdCl_2(chxn)_2](ClO_4)_4$ were recorded at room temperature by applying proton decoupling using a Bruker MSL-300 spectrometer. The chemical shifts given in ppm are relative to external TMS.

(4) (a) Okamoto, H.; Toriumi, K.; Okaniwa, K.; Mitani, T.; Yamashita, M. *Mater. Sci. Eng.* **1992**, *B13*, L9. (b) Huckett, S. C.; Scott, B.; Love, A. P.; Donohoe, R. J.; Burns, C. J.; Garcia, E.; Frankvom, T.; Swanson, B. I. *Inorg. Chem.* **1993**, *32*, 2137. (c) Scott, B.; Berkey, M.; Swanson, B. I. *Chem. Phys. Lett.* **1994**, *226*, 537. (d) Donohoe, R. J.; Worl, L. A.; Arrington, C. A.; Bulou, A.; Swanson, B. I. *Phys. Rev. B* **1992**, *45*, 13185. (e) Matsushita, N.; Kojima, N.; Ban, T.; Tsujikawa, I. *J. Phys. Soc. Jpn.* **1987**, *56*, 3808. (f) Matsushita, N.; Toriumi, K.; Kojima, N. *Mol. Cryst. Liq. Cryst.* **1992**, *216*, 201.

(5) (a) Wada, Y.; Mitani, T.; Yamashita, M.; Koda, T. *J. Phys. Soc. Jpn.* **1985**, *54*, 3143. (b) Wada, Y.; Era, K.; Yamashita, M. *Solid State Commun.* **1988**, *67*, 953. (c) Wada, Y.; Mitani, T.; Toriumi, K.; Yamashita, M. *J. Phys. Soc. Jpn.* **1989**, *58*, 3013. (d) Wada, Y.; Yamashita, M. *Phys. Rev. B* **1990**, *42*, 7398. (e) Iwasa, Y.; Funatsu, E.; Koda, T.; Yamashita, M. *Appl. Phys. Lett.* **1991**, *59*, 2219. (f) Okamoto, H.; Mitani, T.; Toriumi, K.; Yamashita, M. *Phys. Rev. Lett.* **1992**, *69*, 2248. (g) Ooi, H.; Yamashita, M.; Kobayashi, T. *Chem. Phys. Lett.* **1993**, *210*, 384. (h) Kobayashi, T.; Sekikawa, T.; Yamashita, M. *Chem. Lett.* **1997**, 1029. (i) Okamoto, H.; Kaga, Y.; Shimada, Y.; Oka, Y.; Iwasa, Y.; Mitani, T.; Yamashita, M. *Phys. Rev. Lett.* **1998**, *80*, 861. (j) Gammel, J. T.; Saxena, A.; Bishop, A. R.; Batistic, I. *Synth. Met.* **1993**, *54*, 237.

(6) (a) Toriumi, K.; Wada, Y.; Mitani, T.; Bandow, S.; Yamashita, M.; Fujii, Y. *J. Am. Chem. Soc.* **1989**, *111*, 2341. (b) Toriumi, K.; Okamoto, H.; Mitani, T.; Bandow, S.; Yamashita, M.; Wada, Y.; Fujii, Y.; Clark, R. J. H.; Michael, D. J.; Edward, A. J.; Watkin, D.; Kurmoo, M.; Day, P. *Liq. Cryst. Mol. Cryst.* **1990**, *181*, 333. (c) Okamoto, H.; Toriumi, K.; Mitani, T.; Yamashita, M. *Phys. Rev. B* **1990**, *42*, 10381.

(7) (a) Okamoto, H.; Shimada, Y.; Oka, Y.; Chainani, A.; Takahashi, T.; Kitagawa, H.; Mitani, T.; Toriumi, K.; Inoue, K.; Manabe, T.; Yamashita, M. *Phys. Rev. B* **1996**, *54*, 8438. (b) Okamoto, H.; Chainani, A.; Takahashi, T.; Kitagawa, H.; Mitani, T.; Manabe, T.; Yamashita, M. *Synth. Met.* **1997**, *86*, 1977.

(8) Yamashita, M.; Tsuruta, E.; Inoue, K.; Furuta, T.; Okamoto, H.; Mitani, T.; Toriumi, K.; Ohki, H.; Ikeda, R. *Synth. Met.* **1993**, *55*−*57*, 3461.

(9) Yamashita, M.; Inoue, K.; Furuta, T.; Ichikawa, A.; Kimura, N.; Ohki, H.; Ikeda, R.; Kitagawa, H.; Bandow, S.; Toriumi, K.; Mitani, T.; Ohishi, T.; Miyamae, H. *Mol. Cryst. Liq. Cryst.* **1994**, *256*, 179.

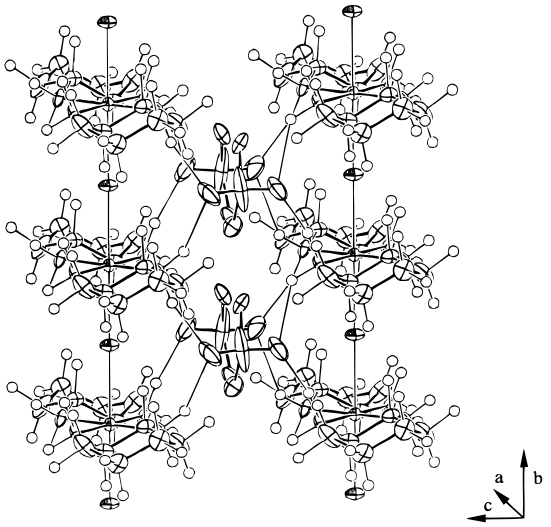

Figure 1. ORTEP drawing of $[Ni(chxn)_2Cl](NO_3)_2$.

The measurements of the XPS and Auger spectra were performed using ESCALAB MK II (VG Scientific Co.) photoelectron spectrometer with Mg Kα ($h\nu$ = 1253.6 eV) or Al Kα ($h\nu$ = 1486.6 eV) as an excitation light source. In these measurements, all samples were ground into powder form in a N_2-gas-filled glovebox attached to the preparation chamber and inserted into the high-vacuum chamber without exposure to air. The base pressure of the analysis chamber was in the 10^{-10} Torr range. The excitation light was operated at low power because the samples degraded on prolonged exposure at high incident power, as observed by the broadening of the Ni 2p core-level spectra. The Fermi level of the sample was determined by referring to that of silver sample.

For the measurements of the polarized reflection spectra, a halogen−tungsten incandescent lamp was used. Light from the lamp was focused by a concave mirror on the entrance slit of a 25 cm grating monochromator (JASCO CD-25). The monochromatic light from the exit slit was passed through a polarizer and was focused on the specific surface of a single-crystal sample by using an optical microscope. Reflected light from the sample was focused by a concave mirror on the detector (a PbS cell or a photomultiplier tube).

Magnetic susceptibilities of polycrystalline samples were measured on a Quantum Design SQUID magnetometer in an applied magnetic field of 2000 G from 2 to 300 K with rising temperature after cooling in a nearly zero magnetic field.

Electrical conductivities of single crystals were measured by using four-probe methods between 165 and 300 K. Carbon paste was used for adhering samples to gold wires.

Results and Discussions

The crystal structures of $[Ni(chxn)_2Cl](NO_3)_2$ are isomorphous to $[Ni(chxn)_2Br](NO_3)_2$, $[Ni(chxn)_2X]X_2$ (X = Cl and Br), and $Ni(chxn)_2Cl_xBr_y$ so far reported[6,8,9] and, moreover, to the mixed-valence compounds $[M^{II}(chxn)_2][M^{IV}(chxn)_2X_2]Y_4$ (M = Pt and Pd; X = Cl, Br, and I; Y = X and ClO_4) although the positions of the bridging halogens are different from one another.[10] The chain structure of $[Ni(chxn)_2Cl](NO_3)_2$ is shown in Figure 1. The relevant bond distances of these compounds are listed in Table 2, along with those of $[Ni(chxn)_2Br](NO_3)_2$, $[Ni(chxn)_2X]X_2$ (X = Cl and Br), and $Ni(chxn)_2Cl_xBr_y$ for comparison. The four N atoms of the two chxn are coordinated to a Ni atom in a planar fashion. The $Ni(chxn)_2$ moieties, lying on special position 222, are bridged by halogen atoms and stacked along the *b* axis, constructing linear-chain structures. The neighboring $Ni(chxn)_2$ moieties along the chain are linked by the hydrogen bonds between aminohydrogens and counteranions, and moreover, there are the hydrogen bonds among the neighboring chains, constructing the two-dimensional hydrogen bond networks parallel to the *bc* plane. In the compounds of $[Ni(chxn)_2Cl](NO_3)_2$, the intra- and interchain hydrogen bonds are composed of NH···O···HN and NH···O−N−O···HN systems, respectively, and the oxygen atom of NO_3^- without incorporation with the interchain hydrogen bonds between the amino hydrogens and NO_3^- is disordered into the upper and lower sides with half occupation. As described previously, in the compounds of $Ni(chxn)_2Cl_xBr_y$, the occupancy factors of Cl and Br ions in the bridging and counteranion positions were determined by the full-matrix least-squares refinements. The occupancy factors of Cl and Br at the bridging halogen sites are 0.976 and 0.024 for $Ni(chxn)_2Cl_{2.459}Br_{0.541}$ (1) and 0.68 and 0.32 for $Ni(chxn)_2Cl_{1.28}Br_{1.72}$ (2), respectively, and those at the counter halogen sites are 1.483 and 0.517 for (1) and 0.60 and 1.40 for (2), respectively. Accordingly, their formula can be correctly represented as $[Ni(chxn)_2Cl_{0.976}Br_{0.024}]Cl_{1.483}Br_{0.517}$ for (1) and $[Ni(chxn)_2Cl_{0.68}Br_{0.32}]Cl_{0.60}Br_{1.40}$ for (2).[8]

To discuss their electronic structures, it is essential to decide whether the bridging halogens are located at midpoints between the two neighboring Ni atoms ($Ni^{III}-X-Ni^{III}$ structure) or deviated from the midpoints ($Ni^{II}\cdots X-Ni^{IV}-X$ structure). On the basis of the careful consideration of the X-ray diffraction, we concluded that these Ni compounds have the $Ni^{III}-X-Ni^{III}$ structures or SDW states. First, their $Ni^{III}-X$ distances are significantly shorter than those of the discrete octahedral Ni^{III} compounds, $[Ni^{III}X_2([14]aneN_4)]ClO_4$ (X = Cl and Br).[11] Second, the structure analyses of these compounds do not indicate positional disorders of the bridging halogen atoms. The thermal ellipsoids of the bridging halogen atoms are very small. Finally, neither diffuse scattering nor satellite peak relating to a superstructure has been observed on the X-ray oscillation and Weissenberg photographs of these compounds.

The *b* axis and *c* axis are correspondent with the $Ni^{III}-X-Ni^{III}$ distance along the chain and the interchain distance in the direction of the hydrogen bonds, respectively. These two axes are systematically influenced with the substitution of the bridging halogens and counteranions. The *b* axes in the $Ni(chxn)_2Cl_xBr_y$ increase in the order of $[Ni(chxn)_2Cl]Cl_2$ < $[Ni(chxn)_2Cl_{0.976}Br_{0.024}]Cl_{1.483}Br_{0.517}$ < $[Ni(chxn)_2Cl_{0.58}Br_{0.32}]Cl_{0.60}Br_{1.40}$ < $[Ni(chxn)_2Br]Br_2$, which is due to the increase of the amounts of Br ions with larger ionic radius. Next, to investigate the effect of the counteranions of NO_3^- and halogen ions (X^-) on the *b* and *c* axes, we compare $[Ni(chxn)_2X](NO_3)_2$ with $[Ni(chxn)_2X]X_2$ (X = Cl and Br). While the $Ni^{III}-X$ or $Ni^{III}-X-Ni^{III}$ distances (*b* axis) are almost similar in the same bridging halogens, the *c* axes of the NO_3^- compounds are much larger than those of X^- compounds, which is due to the larger ionic radius of NO_3^- compared with those of X^-. The correlation between the *b* axis and *c* axis is shown in Figure 2. It can be seen that the $Ni^{III}-X-Ni^{III}$ distances or *b* axes are dependent on the species of bridging halogens and almost constant in the same bridging halogens. This is due to the tight covalent bonds of $Ni^{III}-X-Ni^{III}$. Unfortunately, we could not obtain single crystals of $Ni(chxn)_2X(ClO_4)_2$ (X = Cl and Br) and $Ni(chxn)_2Cl(BF_4)_2$. Therefore, we obtained their crystal parameter such as the *a*, *b*, and *c* axes by using X-ray powder patterns, since their structures are also isomorphous to the $Ni(chxn)_2X_3$ whose crystal structures were determined by single-crystal X-ray diffraction methods. The correlations between *b* and *c* axes are also shown

(10) (a) Larsen, K. P.; Toftlund, H. *Acta Chem. Scand.* **1977**, *31*, 182. (b) Wada, Y.; Lemmer, U.; Gobel, E. O.; Yamashita, M.; Toriumi, K. *Phys. Rev. B* **1995**, *52*, 8276.

(11) Ito, T.; Sugimoto, M.; Toriumi, K.; Ito, H. *Chem. Lett.* **1980**, 1477.

Table 2. Crystal Parameters and Bond Distances (Å)

	a	*b*	*c*	Ni−X	Ni−N
$Ni(chxn)_2Cl_3$	23.975(5)	4.894(1)	6.913(1)	2.447(1)	1.944(1)
$Ni(chxn)_2Cl_{2.459}Br_{0.541}$	23.901(1)	4.914(1)	6.971(1)	2.457(1)	1.939(2)
$Ni(chxn)_2Cl(NO_3)_2$	22.990(20)	4.982(3)	8.001(5)	2.491(1)	1.927(7)
$Ni(chxn)_2Cl_{1.28}Br_{1.72}$	23.720(2)	5.063(1)	7.189(1)	2.531(1)	1.948(3)
$Ni(chxn)_2Br_3$	23.587(5)	5.161(2)	7.121(1)	2.578(1)	1.944(3)
$Ni(chxn)_2Br(NO_3)_2$	22.906(3)	5.213(1)	7.855(1)	2.6065(5)	1.937(4)

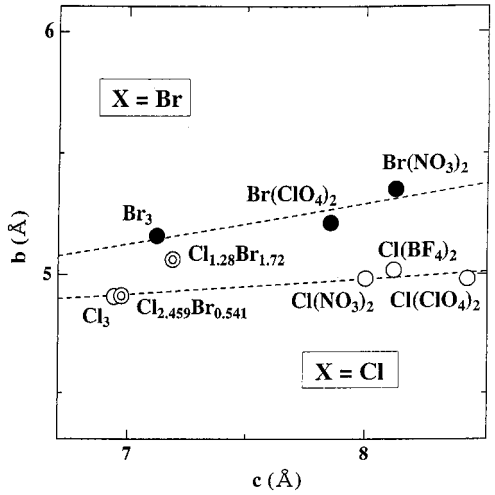

Figure 2. Correlation between *b* and *c* axes in $[Ni(chxn)_2X]Y_2$. The open circles show the chlorobridged compounds, the black circles show the bromobridged compounds, and the double circles show the mixed halide-bridegd compounds.

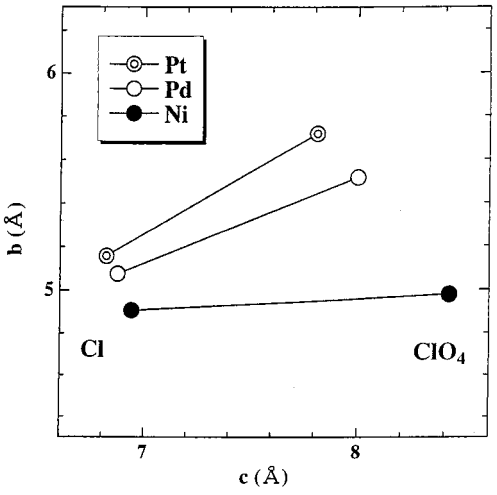

Figure 3. Correlation between *b* and *c* axes in $M(chxn)_2ClY_2$. The double circles show the Pt compounds, the open circles show the Pd compounds, and the black circles show the Ni compounds.

in Figure 2. The *b* axes or $Ni^{III}-X-Ni^{III}$ in the same bridging halogens are almost constant, while the *c* axes or the distances in the direction of the interchain hydrogen bonds are remarkably lengthened in the order X < NO_3 < BF_4 < ClO_4 as the counteranions. Such a trend is consistent with the order of the ionic radius of counteranions. That is, since the $Ni^{III}-X-Ni^{III}$ covalent bonding is tight, the larger counteranions cannot approach the chains, resulting in lengthening of the *c* axes.

At this stage, it is very interesting to compare the correlation between the *b* and *c* axes in the Ni compounds with those in the Pd and Pt compounds in the systems of $M(chxn)_2ClY_2$ (Y = Cl^- and ClO_4^-), where the Ni compounds take Ni^{III} states (SDW States), and the Pt and Pd compounds take $M^{II}-M^{IV}$ mixed-valence states (CDW states). The correlation is shown in Figure 3. Going from Y = Cl to ClO_4 in the Pt compounds, both the *b* and *c* axes are lengthened, where while the $Pt^{IV}-Cl$ distances in both compounds are almost constant, the $Pt^{II}\cdots Cl$ distance in the ClO_4 compound is much longer than that in Cl compounds.[10] The *c* axis in the ClO_4 compounds is much larger than that in the Cl compound, due to the difference of their ionic radius and the hydrogen bond systems. A similar trend is also observed in the Pd compounds, but the degree of the inclination is smaller than that of the Pt compounds. Such results are reasonable from the viewpoint of the intervalence interaction. Because the interaction or overlapping of orbitals between Pd^{II} and Pd^{IV} atoms through the bridging halogens is larger, judging from the results of intervalence CT bands and electrical conductivities, the $Pd^{II}\cdots Cl-Pd^{IV}$ distance or *b* axis is shortening. Then, since the counteranion of ClO_4 cannot approach to the chain, the *c* axis results in lengthening compared with the Pt compounds. In the Ni compounds, such trends are more prominent compared with the Pt and Pd compounds, as shown in Figure 3, due to the tight covalent bonding of $Ni^{III}-Cl-Ni^{III}$.

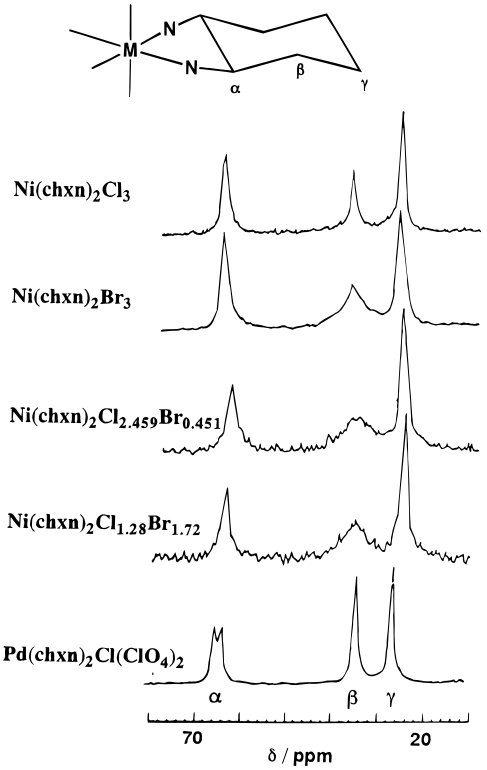

Figure 4. ^{13}C NMR spectra of $[Ni(chxn)_2X]Y_2$ and $Pd(chxn)_2Cl(ClO_4)_2$.

^{13}C NMR spectra of $Ni(chxn)_2X_3$ (X = Cl, Br, and mixed halides) observed at room temperature exhibited three resonance lines with almost integrated intensity as shown in Figure 4. These results are in good agreement with the crystal structural data, revealing the presence of three kinds of crystallography-cally independent carbon atoms of the chxn ligands in the crystals, namely, α-, *β*-, and *γ*-carbons.

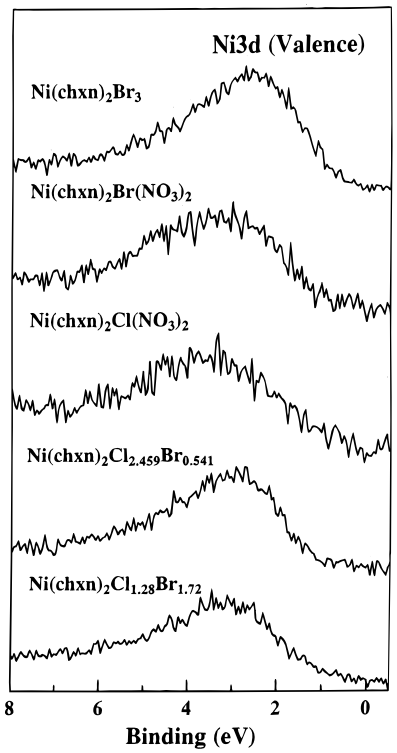

Figure 5. Valence-band XP spectra of $[Ni(chxn)_2X]Y_2$.

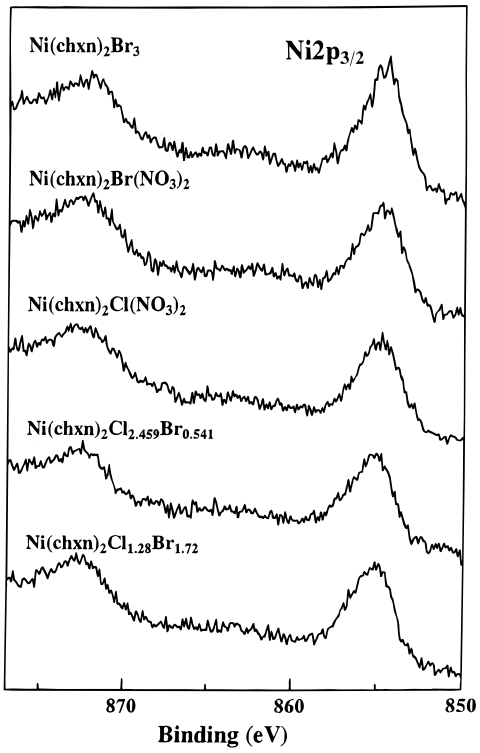

Figure 6. Ni 2p XP spectra of $[Ni(chxn)_2X]Y_2$.

To estimate the on-site Coulomb energies of these compounds, we have measured their Auger spectra and XP spectra. Figure 5 shows the valence-band XP spectra of the Ni compounds, which were obtained by using Mg Kα radiation. In the spectra, the broad peaks centered at 3−4 eV binding energies are observed. Both Ni 3d and bridging halogen 3p(Cl) or 4p(Br) electrons will contribute to the XPS intensities in this region. Since the XPS cross section of the Ni 3d electrons is comparatively larger than those of Cl 3p and Br 4p electrons for the Mg Kα radiation, the broad peak at 3−4 eV can be considered to have a dominantly 3d character. The Ni 2p XP spectra obtained using Mg Kα radiation are shown in Figure 6. The spectra are composed of the two peaks, that is, Ni $2p_{3/2}$ and Ni $2p_{1/2}$, where the former is observed in the higher energy region compared with the latter. These binding energies are higher than those in the Ni^{II} complexes. To evaluate the electron−electron correlation between the 3d electrons *U*, the Ni LVV Auger spectra have been measured. Figure 7 shows the Auger spectra which are obtained by Al Kα radiation, since the strong N 1s XP line appears in the Auger spectral region with the excitation of the Mg Kα radiation. From these results, the *U* values are obtained by using the equation described previously.[7] All results are listed in Table 3. The *U* values in these compounds are about 5 eV, which are almost equal to those of $[Ni(chxn)_2X]X_2$ reported previously.

The optical conductivity spectra of the single crystals of these compounds are shown in Figure 8, which were obtained by the Kramers−Kronig transformation from the polarized reflectivity spectra with the electric vector **E** parallel to the chain axis *b* (E ∥ *b*). In the energy region from 1.2−2.0 eV, the prominent absorptions are observed in these compounds, where are polarized parallel to the chain axis *b*, but no prominent structures are observed for the E ⊥ *b* spectra. Their peak energies are listed in Table 3. As mentioned above, the on-site Coulomb energies are estimated to be about 5 eV. On the other hand, the lowest transitions are observed in the energy regions from 1.2 to 2.0

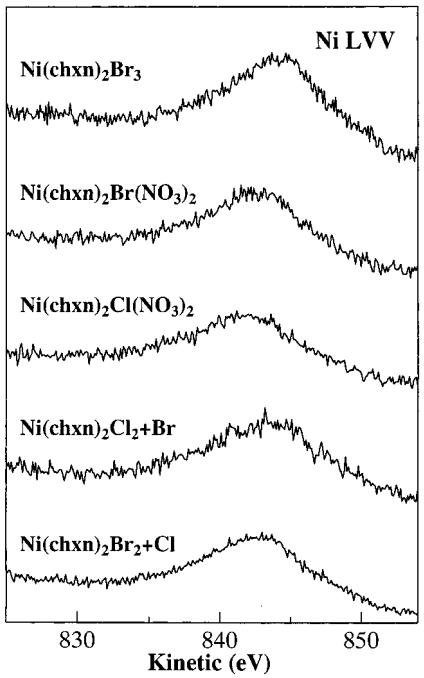

Figure 7. Ni LVV Auger spectra of $[Ni(chxn)_2X]Y_2$.

eV. Therefore, the lowest transitions are considered as those of the bridging halogens to the upper Hubbard bands of the Ni $3d_{z^2}$. Then, these compounds are not Mott-insulators but CT-insulators, where the energy levels of the bridging halogens are located between the lower and upper Hubbard bands composed of the Ni^{III} $3d_{z^2}$ orbitals. The peak energies shift in the order of $Ni(chxn)_2Cl_3 > Ni(chxn)_2Cl_{2.459}Br_{0.541} > Ni(chxn)_2Cl_{1.28}Br_{1.72} > Ni(chxn)_2Br_3$, which is well interpreted by the energy difference of the 2p of Cl and 3p of Br ions. In the same bridging halogens, the peak energies of the NO_3^- compounds are higher than those of the halogen counteranions, which is due to slightly longer $Ni^{III}-X-Ni^{III}$ distances in the NO_3^- compounds.

Table 3. Electron Correlations (U), CT Peak Energies, and Electrical Conducting Data

	U (eV)	E_{CT} (eV)	E_a (eV)	log σ (S cm^{-1})
$Ni(chxn)_2Cl_3$	~4.47	1.95	0.302	−6.61
$Ni(chxn)_2Cl_{2.459}Br_{0.541}$	~5.95	1.75	*a*	*a*
$Ni(chxn)_2Cl_3$	~4.9	1.80	0.232	−6.00
$Ni(chxn)_2Br(NO_3)_2$	~5.91	1.45	0.178	−5.61
$Ni(chxn)_2Cl_{1.28}Br_{1.72}$	~5.35	1.45	0.137	−4.73
$Ni(chxn)_2Br_3$	~5.84	1.28	0.117	−3.16

[a] Single crystals are too small to be measured.

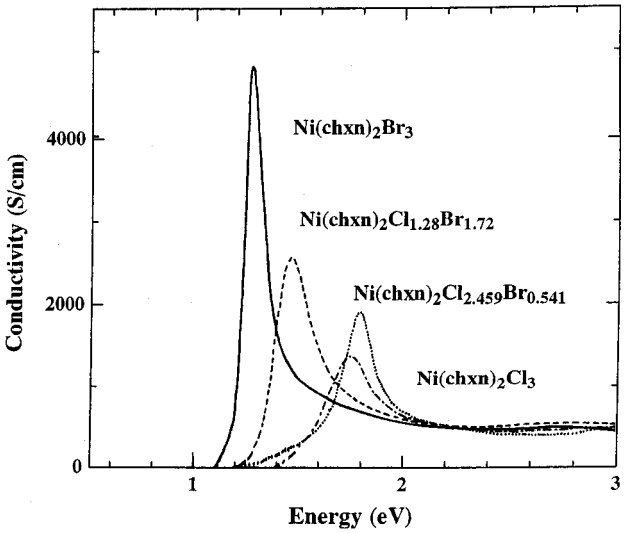

Figure 8. Optical conductivity spectra of the single crystals of $[Ni(chxn)_2X]Y_2$.

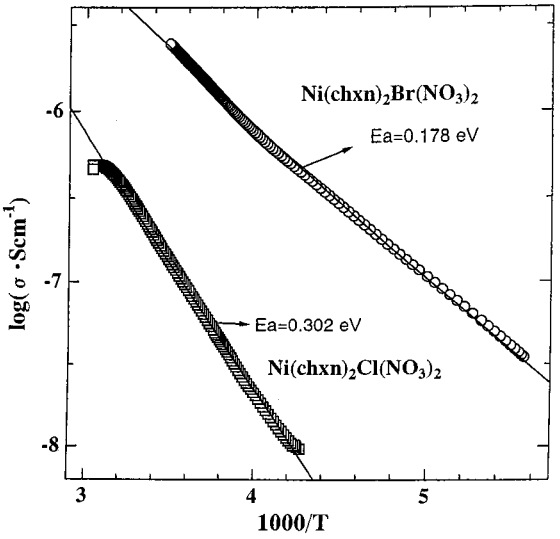

Figure 9. Single-crystal electrical conductivities of $[Ni(chxn)_2X](NO_3)_2$.

Single-crystal electrical conductivities have been measured along the chain axes by the four-probe method (Figure 9). All these compounds show semiconducting behaviors. All data are listed in Table 3, where the resistivities at room temperature and the activation energies increase in the order of $Ni(chxn)_2Br_3$ < $Ni(chxn)_2Cl_{1.28}Br_{1.72}$ < $(Ni(chxn)_2Cl_{2.459}Br_{0.541})$ < $Ni(chxn)_2Cl_3$, and in the same bridging halogens those of the NO_3^- compounds are larger than those of halogen counteranion compounds. Such orders are the same as those of the peak energies of the charge-transfer bands.

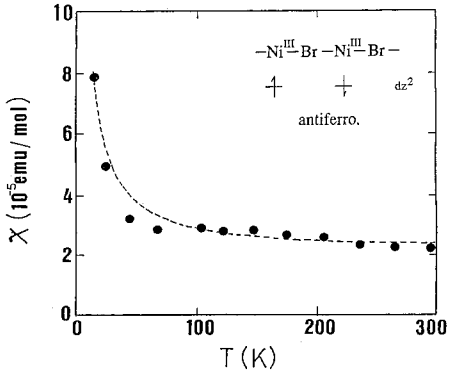

Figure 10. Temperature dependence of magnetic susceptibility of $[Ni(chxn)_2Br]Br_2$. The dashed line represents the linear combination of the Bonner−Fisher curve and Curie curve (0.22%).

The temperature-dependent magnetic susceptibility measurements reveal that all these compounds show the very strong antiferromagnetic interactions, which are due to the superexchange mechanism through the bridging halogens between neighboring spins located on the Ni $3d_{z^2}$ (Figure 10). The exchange parameters $|J|$ are estimated to be 1150 K for $Ni(chxn)_2Cl(NO_3)_2$, 1200 K for $Ni(chxn)_2Cl_3$, 1500 K for $Ni(chxn)_2Br(NO_3)_2$, and 1700 K for $Ni(chxn)_2Br_3$ by using the Bonner−Fisher equations. The negative linear correlation between the magnitudes of $|J|$ and the peak energies of the CT bands are observed. This is well interpreted with the superexchange interactions through the bridging halogen ions between neighboring Ni^{III} ions.[12]

Conclusion

New quasi-one-dimensional halogen-bridged Ni^{III} compounds, $[Ni(chxn)_2X]Y_2$ have been synthesized by chemical and electrochemical methods. Judging from the results of crystal structures, XPS, Auger spectra, and single-crystal optical measurements, these compounds are CT-insulators, where the energy levels of the bridging halogens are located between the upper and lower Hubbard bands. Therefore, their electronic structures are very similar to those of the starting materials of the copperoxide supperconductors. It is founded that the SDW strengths in these compunds can be tuned by substituting the bridging halogens and the counteranions.

Acknowledgment. We thank Professor K. Nasu (KEK) for valuable discussions. This work was partly supported by a Grant-in-Aid for Science Research from the Ministry of Education, Science and Culture, Japan.

Supporting Information Available: X-ray crystallographic data for $[Ni(chxn)_2Cl](NO_3)_2$ including tables of atomic coordinates, bond angles, and bond lengths. This material is available free of charge via the Internet at http://pubs.acs.org.

IC9812499

(12) Okamoto, H.; Yamashita, M. Manuscript in preparation.